*Proceedings of the Eighth European Conference*
*on Underwater Acoustics, 8th ECUA*
Edited by S. M. Jesus and O. C. Rodríguez
Carvoeiro, Portugal
12-15 June, 2006

# MODELING DOPPLER-SENSITIVE WAVEFORMS MEASURED OFF THE COAST OF KAUAI

Martin Siderius[1], Michael B. Porter[1], Paul Hursky[1] and Vincent McDonald[2]

[1]HLS Research Inc., San Diego, CA
[2]Space and Naval Warfare Systems Center, San Diego, CA

Abstract: Predicting underwater acoustic communications performance in previously untested environments requires accurate modeling of the channel in both a static and dynamic sense. In this paper, a simple technique is presented for modeling high-frequency, broadband acoustic signals including Doppler effects. Modeled results are compared with measurements from Doppler sensitive transmissions taken with both towed and moored sources off the coast of Kauai during the 2005 Makai experiment. The measured data show a clear but somewhat complicated pattern of Doppler shift, varying for each subsequent arrival. The resulting pattern is interpreted and modeled as a combination of effects due to vertical and horizontal velocity components introduced through surface and source/receiver motion.

## 1. INTRODUCTION

For many sonar applications, ignoring the slight Doppler shift introduced by platform motion has little impact on performance. However, for underwater acoustic communications systems, compensating for Doppler effects can present a substantial challenge. In particular, channel equalizers used with bandwidth-efficient, phase-coherent methods can be extremely sensitive to Doppler spread. Significant Doppler spread can be introduced simply from the sound interacting with the moving sea-surface; however, the effects are much greater when the source and receiver are also in motion. Simulating communication signals using a physics-based model can greatly aid the development of new algorithms and provide valuable performance predictions. A simple technique for modeling high-frequency, broadband acoustic signals in the ocean that includes Doppler effects will be described in Section 2. The original motivation for this work was to simulate active sonar receptions on moving marine mammals— here it is applied to acoustic communications [1].

The relatively high frequencies (e.g. 3-50 kHz) and broadband signals widely used for communications suggest using Gaussian beam tracing. One of the attractive fea-

tures of this method is the ability to simulate broadband signals with a single ray/beam trace. Further, Gaussian beams are conveniently interpolated and extrapolated to allow for the treatment of Doppler effects due to environmental and/or source/receiver motion. Receptions from towed and fixed source during the 2005 Makai experiment will be compared with the simulations. Relevant details of the 2005 Makai experiment will be briefly described in Section 3.

## 2. MODEL DESCRIPTION

The complex pressure field, $P(\omega)$, can be represented as a sum of $N$ arrival amplitudes $A_n(\omega)$ and delays $\tau_n(\omega)$ according to,

$$P(\omega) = S(\omega) \sum_{n=1}^{N} A_n e^{i\omega\tau_n}, \tag{1}$$

where $S(\omega)$ is the spectrum of the source. Several ray and beam tracing computer codes could be used to compute amplitudes and delays, but here the Gaussian Beam Tracing code implemented in Bellhop is used [2].

According to the convolution theorem, the product of two spectra is a convolution in the time domain. This leads to the time-domain representation for the received waveform, $p(t)$, which can be written:

$$p(t) = \sum_{n=1}^{N} A_n s(t - \tau_n). \tag{2}$$

where $s(t)$ is the source waveform. This representation is intuitive, with the received sound being a sum of echoes with various amplitudes and delays. However, these amplitudes are generally complex numbers due to arbitrary phase shifts that occur from bottom reflections. This will erroneously produce a complex $p(t)$ in eq. (2).

The convolution theorem can be recast to consider the complex amplitudes and the conjugate-symmetry of $P(\omega)$. This will guarantee a real received waveform. The proper convolution sum is then:

$$p(t) = \sum_{n=1}^{N} \mathrm{Re}\{A_n\} s(t - \tau_n) - \mathrm{Im}\{A_n\} s^{+}(t - \tau_n). \tag{3}$$

where $s^{+} = \mathcal{H}(s)$ is the Hilbert transform of $s(t)$. The Hilbert transform is a 90° phase shift of $s(t)$ and accounts for the imaginary part of $A_n$. Equation (3) can be interpreted as saying that any arbitrary phase change can be understood as a weighted sum of the original waveform and its 90° phase-shifted version. The weighting controls the effective phase shift.

In this approach, the boundary reflection coefficients have been assumed to be independent of frequency. While this is true for homogeneous bottom types (i.e. half-space) it is not strictly true when the bottom is layered or has sound-speed gradients. As an illustration of the frequency dependence (or lack of) on beam/ray arrivals, we consider an iso-sound speed ocean (1500 m/s) environment with 100 m water depth (source depth is 30 m and receiver depth is 60 m at 1 km range). In Fig. 1 the bottom reflection loss is shown for 8 and 16 kHz along with the corresponding arrival amplitudes and phase. Note

that the results for the two frequencies would be identical if a half space were used. In this case, a layered seabed has been introduced to highlight the frequency dependence. The seabed consists of a 1-m layer of fine sand (1660 m/s) over sandy-gravel (2000 m/s). Even in this layered case many of the arrivals have exactly the same amplitude and delay. Some of the weaker, late arrivals show slight differences depending on the number of bottom bounces. While frequency dependence can be introduced by fine-scale variations in the

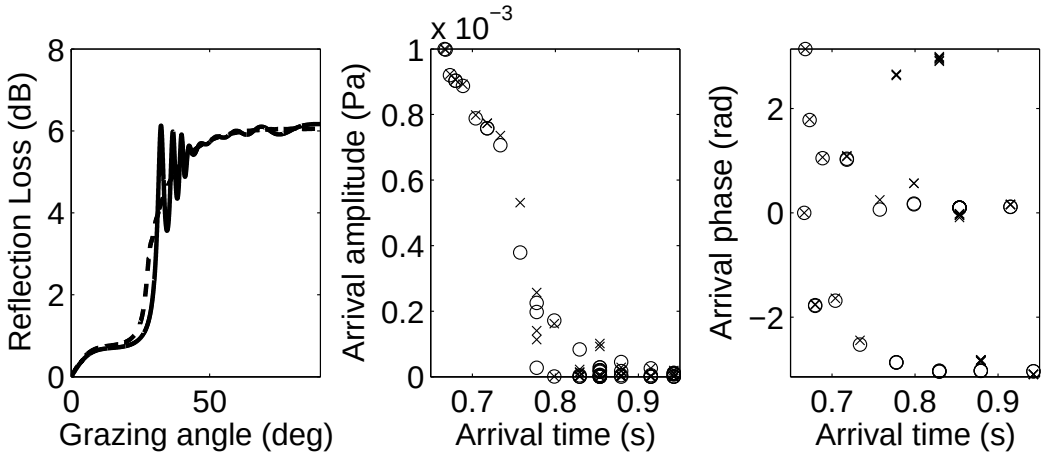


*Fig. 1 Left panel shows the bottom reflection loss for 8 (dashed) and 16 kHz. Middle panel shows the corresponding arrival amplitudes (8 kHz circles) the right panel shows the phase.*

seabed these are often not known in sufficient detail (on the sub-meter scale) to include in modeling. A single sound speed, density and attenuation is often a good approximation at communications frequencies. A summary of seabed properties for these and other seabed types can be found in Ref. [3].

The approach described can be modified to accommodate a moving receiver. Imagine stationary receivers positioned at every possible location in the environment and each recording its received time-series. As the moving receiver proceeds through the environment, at each time-step it samples the response from the time-series of the stationary receiver corresponding to its current location. In practice, computing the full time-series on a dense grid of receivers is impractical. Fortunately, the entire time-series for each stationary receiver does not need to be computed; it is only computed for the time-step the moving receiver samples. The end result is equivalent to the moving receiver having time-dependent amplitudes and delays. Equation (3) is then cast in terms of these time varying amplitudes and delays:

$$p(t) = \sum_{n=1}^{N} \mathrm{Re}\{A_n(t)\} s[t - \tau_n(t)] - \mathrm{Im}\{A_n(t)\} s^{+}(t - \tau_n(t)). \tag{4}$$

Using Eq. (4) requires computing the amplitudes and delays on an incredibly fine spatial grid. This degree of spatial sampling is not very practical; however, using a Gaussian Beam approach allows for spatial interpolation and extrapolation of arrival amplitudes and delays. This is possible since arrival patterns vary slowly over spatial scales of several

to hundreds of wavelengths. One difficulty often encountered with arrival interpolation is the so-called ray identification problem. That is, to calculate the field between grid points, the same arrival type (i.e. direct path, surface bounce etc.) needs to be identified before interpolating its amplitude and phase. This sounds simple enough but can be problematic since arrivals on one grid point may not correspond to those at another. That is, reflection and refraction can cause both a different number of rays and different ray-types on each of the grid points. For example, consider the direct path on one grid point that is refracted away from another grid point. In this case, interpolating the first arrival between these grid points may involve interpolation of a direct path with a bottom-bounce path and this will produce incorrect results.

This problem can by avoided without keeping track of arrival types by using an approach similar to using shape functions in finite-element methods. The influence of these shape functions can be computed independently but their sum provides the equivalent of a bilinear interpolation. Consider a rectangular grid with receiver location somewhere in the middle of four grid points. The amplitudes at the grid points are maintained as separate quantities and their corresponding delays are adjusted by the ray path travel-time differences between the grid point and the receiver location. The amplitudes are adjusted by the appropriate travel distance. The received field is constructed using Eq. (4) with an additional sum over each of the arrivals on the four grid points. The weight given to each grid point is based on bi-linear interpolation. In other words, the arrivals are never interpolated between grid points. In this way, sorting and interpolating based on arrival types is not necessary and results are surprisingly good. Surface motion can be treated in this manner by extending the interpolation. This adds another dimension to Eq. (4), and results in the sum being calculated over arrivals on eight grid points.

## 3. THE MAKAI EXPERIMENT

The Makai experiment took place from September 15 to October 1, 2005 near the coast of Kauai, HI [4]. The site has a coral sand bottom with a fairly flat bathymetry that was nominally 100 m. The water column was variable but typically had a mixed layer depth of 40-60 m and was downward refracting below. The data was measured on September 24th using both stationary and towed sources (from R/V *Kilo Moana*). The sources were programmable, research modems developed at SPAWAR Systems Center (referred to as the Telesonar Testbeds [5]). Signals were received on the AOB2 array, an autonomous system developed at the University of Algarve, Portugal. The AOB2 is a drifting 8-element self-recording array that resembles the size and weight of a standard sonobuoy; details on the AOB2 array can be found in Ref. [6]. The experiment geometry and bathymetry is shown in the left panel of Fig. 2. The right panel of Fig. 2 shows a ray trace of the T1-AOB acoustic paths. The paths are numbered on the figure and correspond to (1) direct, (2) surface bounce (3) bottom bounce (4) surface-bottom bounce (5) bottom-surface bounce. The different path directions have sensitivity to different velocity components. The higher numbered paths are more Doppler sensitive to the vertical velocity components and the lower numbered paths (e.g. direct path) are more sensitive to the horizontal velocity components.

A 0.7 s BPSK (binary-phase-shift-keying) transmission was used for the analysis [7]. This waveform is commonly used for communications but for this analysis is simply a

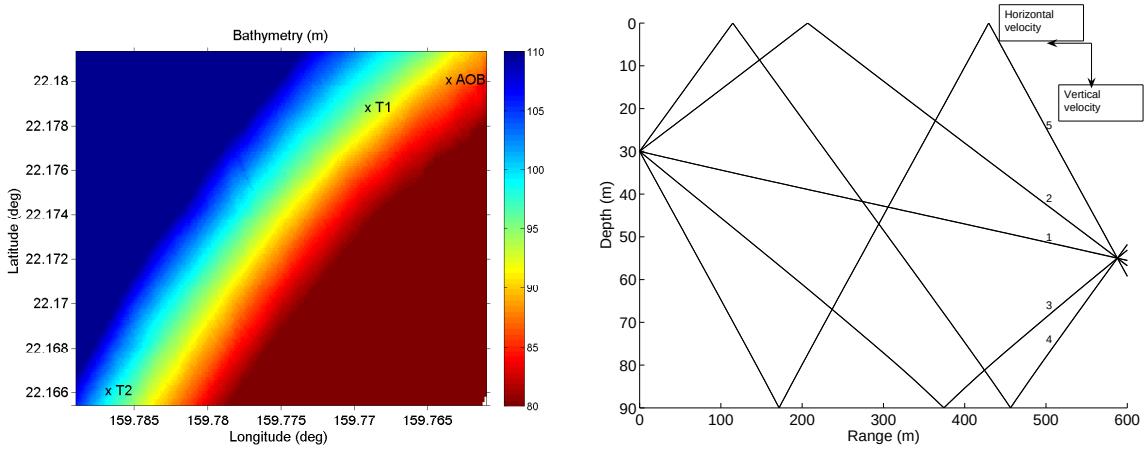


*Fig. 2 Left panel: Bathymetry near Kauai with the positions of the AOB vertical array and the Telesonar Testbeds T1 and T2 at 01:00 on JD 268. T1 was about 600 m away from AOB and being towed while T2 is about 2.8 km away and is stationary. Right panel: Ray trace between testbed T1 and the AOB array. The various paths are labeled (1) direct, (2) surface bounce (3) bottom bounce (4) surface-bottom bounce (5) bottom-surface bounce.*

highly Doppler-sensitive signal [7]. The transmission used cycles of a 9.5 kHz sinusoid with phase shifts introduced to represent a string of 1's and 0's defined by an m-sequence [7]. In a static situation, using a matched filter on this waveform produces an estimate of the channel impulse response. However, in situations with source/receiver motion, each path can have a different Doppler shift (due to the angle-dependent propagation paths). A single Doppler shift can be applied to the BPSK transmit signal before the matched filter process. By sweeping over a variety of shifts the Doppler for each received arrival can be estimated. The resulting picture is closely related to the so-called channel "scattering-function".

### 3.1 Results

The first transmission considered here had a range separation of 2.8 km between the fixed Testbed T2 and the AOB (JD 268 at 01:04). The second transmission is from the towed Testbed T1 and received on the AOB about 600 m away (JD 268 at 01:02). The receptions are shown in Fig. 3. The bright spots indicate an arrival in time along the x-axis. (Note, only relative time is known so the time series are aligned based on the first arrival and the known distance between source and receiver). The y-axis shows the relative speed that corresponds to the peaks. The left panel is for the stationary T2 and Doppler indicates the AOB was drifting at about 0.1–0.2 m/s (estimate from GPS positions indicated about 0.12 m/s). The first arrivals show decreasing Doppler for the first few arrivals followed by the last visible arrival having an increased Doppler shift. For horizontal velocity one expects the later arrivals to have decreasing Doppler shifts due to higher propagation angles relative to the direction of motion. The high Doppler on the last arrival implies a component in the vertical which would introduce larger shifts for late arrivals.

The right panel of Fig. 3 shows the reception from T1 which was being towed with relative speed between T1 and the AOB of about 1.2–1.4 m/s (estimate from GPS positions is 1.24 m/s). Like the stationary case, Doppler shifts do not decrease monotonically on the steeper paths but, in some cases, increase. The paths can be identified using the ray trace in Fig. 2. The second and fourth arrivals both have *increased* Doppler shifts relative to the direct path while the third arrival has a slightly *decreased* Doppler. Paths two and four correspond to the surface and surface-bottom bounce paths while the third arrival is the bottom bounce.

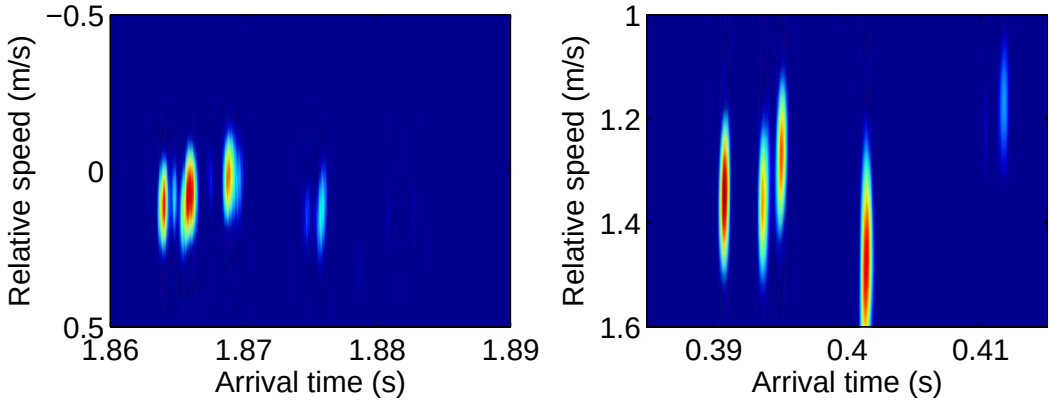


*Fig. 3 Left panel shows the measured impulse response for various Doppler shifts indicated on the y-axis between the drifting AOB and the stationary T2 at 01:04 on JD 268. Each bright spot corresponds to an arrival with delay time shown along the x-axis. The right panel is for a reception from the towed source T1 at 01:02 on JD 268.*

It is critical to correctly identify the paths so that the proper Doppler mechanism is attributed. That is, Doppler associated with the bottom bounce path can be attributed to receiver motion but not to surface motion while a surface bounce path can have Doppler contributions from both. A sanity check on the geometry can be made by comparing the array response on the AOB to a modeled response for the assumed geometry (i.e. water depth, source depth, array depth). The data is matched filtered for a variety of Doppler shifts and the maximum for each arrival is selected. The results are shown in Fig. 4 where individual arrivals are resolved. The modeled impulse response uses a static environment and shows a similar arrival pattern.

The transmission for the towed testbed, T1, to the AOB was first modeled for Doppler with a horizontal velocity of 1.3 m/s. This result is shown in panel (b) of Fig. 5 with the measured data shown in panel (a) (same as right panel of Fig 3). Modeling only horizontal velocity does not show particularly good agreement with the measurements (comparing (a) with (b)). In panel (c) of Fig. 5, a slight receiver vertical velocity component of 0.12 m/s is included in the modeling and this gives approximately the correct shift to the third path (bottom bounce) but does not adequately capture the shifts seen on the second and fourth arrivals. To better model the data the surface was assumed to be moving vertically at 0.5 m/s and this combined Doppler model is shown in panel (d) of Fig. 5. The combined model in (d) still fails to captures the fifth arrival which indicates more complicated surface motion.

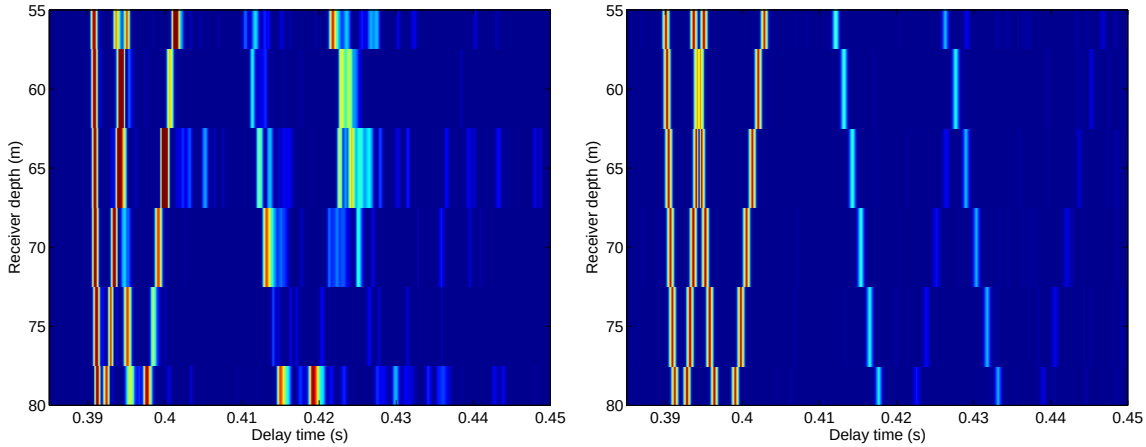


*Fig. 4 Left panel: impulse response on the AOB array with optimal Doppler correction for each path. Delay times for arrivals are shown along the x-axis for various depths (y-axis). Right panel: modeled (static) impulse response for the assumed geometry.*

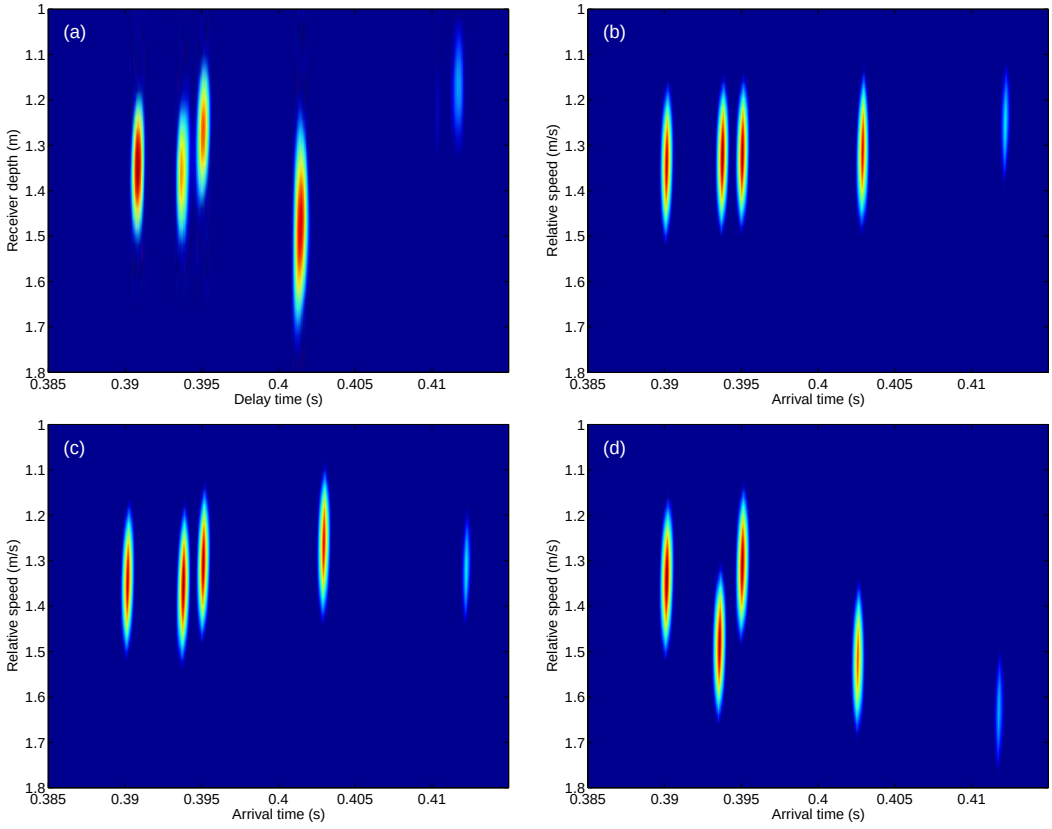


*Fig. 5 (a) Measured arrivals between the AOB and T1 (same as right panel of Fig. 3) (b) Simulated arrival pattern including velocity only in the horizontal (range) direction (1.3 m/s) (c) Simulated with inclusion of vertical (0.12 m/s) and horizontal velocity components on receivers (d) Simulated with inclusion of surface motion (0.5 m/s).*

## 4. CONCLUSIONS

A simple method for modeling path dependent Doppler shifts is described and compared with measurements from Makai, 2005. Correct Doppler modeling is important when designing communications systems and the model-data agreement implies this technique could be used for realistic simulations. The data suggests horizontal and vertical velocity components. The vertical component appears to primarily be due to surface motion with a very slight receiver motion. This type of modeling is useful for testing communications algorithms since there is a high degree of realism. Further, this can be used to determine when/if communications systems will fail when motion is introduced.

## 5. ACKNOWLEDGEMENTS

The authors would like to thank Sergio Jesus, Antonio da Silva and Friedrich Zabel at the Signal Processing Laboratory at the University of Algarve, Portugal for their support and cooperation with the received AOB data used for this analysis.

## REFERENCES

[1] M. Siderius and M. B. Porter, Modeling Techniques for Marine Mammal Risk Assessment. *IEEE Journal of Oceanic Engineeering*, 31, (1), January 2006.

[2] M. B. Porter and Homer P. Bucker, Gaussian Beam Tracing for Computing Ocean Acoustic Fields. *J. Acoust. Soc. Am.* 82, (4), 1349-1359 1987.

[3] APL-UW High-Frequency Ocean Environmental Acoustic Models Handbook. *Tech. Report Appl. Physics Lab.* Univ. of Wash., Seattle WA, USA, APL-UW 9407, 1994.

[4] M. B. Porter, Overview of the Makai Experiment. *Proceedings of the Eighth European Conference on Underwater Acoustics,*, Edited by S. M. Jesus and O. C. Rodriguez, Carvoeiro, Portugal, June 2006.

[5] V. K. McDonald, P. Hursky and the KauaiEx Group, Telesonar Testbed Instrument Provides a Flexible Platform for Acoustic Propagation and Communication Research in the 8–50 kHz Band. *High-Frequency Ocean Acoustics*, Edited by M. Porter, M. Siderius and W. A. Kuperman, AIP, Melville, NY, 2004.

[6] A. Silva, F. Zabel, C. Martins, The Acoustic Oceanographic Buoy Telemetry System—A Modular Equipment that Meets Acoustic Rapid Environmental Assessment Requirements. *Sea Technology*, to appear, September, 2006.

[7] J. G. Proakis, *Digital Communications*, Third Edition, McGraw-Hill, NY, NY.